EFDA–JET–CP(13)03/37

T. Koskela, O. Asunta, P. Belo, M. O'Mullane, M. Romanelli, S. Sipilä
and JET EFDA contributors

Modelling of the Effect of the ITER-like Wall on NBI Heating in JET

Modelling of the Effect of the ITER-like Wall on NBI Heating in JET

T. Koskela[1], O. Asunta[1], P. Belo[4], M. O'Mullane[3], M. Romanelli[2], S. Sipilä[1]
and JET EFDA contributors*

JET-EFDA, Culham Science Centre, OX14 3DB, Abingdon, UK

[1]Aalto University School of Science, PO Box 14100, FI-00076 AALTO, Finland
[2]EURATOM-CCFE Fusion Association, Culham Science Centre, OX14 3DB, Abingdon, OXON, UK
[3]Department of Physics, University of Strathclyde, Glasgow G4 0NG, UK
[4]Associacao EURATOM/IST, IPFN Laboratorio Associado, IST,P-1049-001 Lisboa, Portugal
** See annex of F. Romanelli et al, "Overview of JET Results",*
(24th IAEA Fusion Energy Conference, San Diego, USA (2012)).

Preprint of Paper to be submitted for publication in Proceedings of the
40th EPS Conference on Plasma Physics, Espoo, Finland.
1st July 2013 – 5th July 2013

INTRODUCTION

Following the installation of the ITER-like wall (ILW) at JET, carbon has been replaced by beryllium and tungsten as the main core plasma impurity. Simultaneously, the neutral beams have been upgraded to achieve higher heating power [1]. Understanding if and how the deposition of heating power from the neutral beams has changed with these upgrades will have an impact on the coming JET campaigns and on ITER operation.

In this work we report numerical simulations which study the effect of the upgraded JET NBI and tungsten impurity content on beam deposition.We compare the deposition from the old and the upgraded beam configurations in plasmas with the C-wall and the ILW. Furthermore, we investigate the effect of an asymmetrically distributed tungsten impurity on beam stopping. We use the orbit-following code ASCOT [2], coupled to the JETTO transport code, to calculate the beam deposition including the slowing-down and pitch and scattering of the beam ions. To take into account the effect of tungsten, ASCOT has been updated to use the ADAS database to obtain effective beam stopping coefficients. The results of ASCOT are compared with the PENCIL code, in order to determine the significance of fast ion orbit effects.

To study the effect of the neutral beam upgrade on the beam deposition a set of discharges, summarized in table 1, was selected from the JET core transport database. The set consists of four pairs of similar C wall and ILW shots, and includes pairs of hybrid and baseline shots with high and low triangularity. A time window of 1s where the main plasma parameters were relatively stable was chosen from each shot, and time averaged temperature and density profiles were calculated from HRTS data, assuming $T_i = T_e$. The average value of Z_{eff} was calculated from vertical visible spectroscopy data, and carbon and beryllium were used as impurities.With these steady-state profiles, JETTO was run interpretively, with ASCOT and PENCIL to calculate the beam deposition, using experimental data for the beam voltage and energy fractions. The simulations were then repeated, with the beam parameters and the mix of plasma species swapped between the similar C wall and ILW discharges. We obtain a comparison of the new and the old beams, and for PENCIL and ASCOT, for each discharge.

The calculated fast ion deposition profiles are shown in figure 1(a). The heating power deposited from the beam to the thermal plasma is qualitatively similar to the fast ion density. We can conclude that outside $\rho \approx 0.3$ ASCOT and PENCIL are in good agreement, while ASCOT predicts a higher deposition inside $\rho \approx 0.3$.

The relative difference in deposited fast ion density of post-upgrade NBI to pre-upgrade NBI is shown in figure 1(b). The ASCOT simulations of hybrid scenarios show an identical trend: There is an increase in deposition on axis, then a slight decrease at $\rho \approx 0.3$ and an increase towards the edge. In the corresponding PENCIL simulations the deposition is reduced on-axis and increased at the edge. In the high d baseline scenarios, both codes predict very little change in deposition. In the low d baseline scenario ASCOT predicts an increase in deposition from the axis to $\rho \approx 0.5$, while PENCIL predicts a slight decrease mid-radius, but overall little change. We study the effect

of tungsten on beam attenuation by initializing JETTO/SANCO with a radially constant, fixed value of Z_{eff} with tungsten as the only impurity, and run the simulation using ASCOT to calculate the beam deposition. The simulations show that if a constant Z_{eff} profile is assumed, an unsustainably high tungsten concentration has to be imposed for any noticeable effect on beam attenuation.

However, both theory and observations suggest the density of heavy impurities can be strongly peaked due to a centrifugal force generated by plasma rotation [3]. It can be shown [4] that by assuming a slowly rotating trace impurity, its 2D density profile $n_I(\psi, \theta)$ can be expressed as a function of its flux-surface averaged density $\langle n_I(\psi, \theta)\rangle$ and the toroidal angular frequency Ω as

$$n_I(\psi,\theta) = \langle n_I(\psi,\theta)\rangle \frac{exp\left(\frac{m^*\Omega^2(\psi)}{2T_i(\psi)}R^2(\psi,\theta)\right)}{\left\langle exp\left(\frac{m^*\Omega^2(\psi)}{2T_i(\psi)}R^2(\psi,\theta)\right)\right\rangle}. \quad (1)$$

Here, ψ is the poloidal flux coordinate, θ is a poloidal angle, $m^* = m_I \frac{Zm_iT_e}{T_e+T_i}$, T_i is the ion temperature profile, Z is the impurity charge state, R is the major radius and $\langle f\rangle$ is the flux surface average of f. Since the impurity density peaking will be centered on the outer midplane, we expect this effect to enhance the beam stopping effect of tungsten.

We apply equation (1) to flux-surface averaged profiles, illustrated in figure 3, from JETTO/SANCO modelling of a hybrid low δ Pulse No: 82722 at t =5.9s [5]. We assume that the electron density remains fluxsurface average and the main ion density responds to the redistribution of tungsten to maintain quasineutrality. We also include beryllium as a second impurity to obtain reasonable values of Z_{eff} and radiation, but assume it does not get redistributed by rotation. The obtained tungsten profile is illustrated in figures 2(b) and 2(c), which indicate the peak value of density exceeds the flux-surface averaged value by a factor 4.

We first run ASCOT in steady-state to calculate the beam deposition at t = 5.9s. In terms of flux-surace averaged quantities, we see the effect of the tungsten as a slight decrease in heat deposition inside mid-radius, and slight increase outside. Shine-through is not affected. We calculate the beam-target neutron rate, shown in figure 2(d), and see a decrease of neutrons produced near the magnetic axis and a slight increase near the tungsten peak. The volume integrated neutron rate is reduced by 4%, when the rotation is taken into account.

Finally, we let JETTO/SANCO evolve the impurity profiles in time, and run ASCOT time dependent to capture the evolution of the beam deposition. In our simulation case, the tungsten density decays rapidly, and we cease to see a difference in the neutron rates with and without rotation after approximately 500ms. The result of this simulation is shown in figure 4.

In summary, we have simulated the effect of the JET NBI upgrade and the effect of heavy impurity redistribution by plasma rotation on the neutral beam deposition profiles. The ASCOT code has been upgraded to account for redistribution of heavy impurities by plasma rotation, and the model has been applied to JET Pulse No: 82722. We find local changes of the order 10% to

the fast ion deposition profile, due to the NBI upgrade and the change in the impurity mix. With tungsten concentration of the order 10^{-4} we find a reduction of beam-target neutron rate close to the magnetic axis when rotation is taken into account.

ACKNOWLEDGEMENTS

This work was supported by EURATOM and carried out within the framework of the European Fusion Development Agreement. The views and opinions expressed herein do not necessarily reflect those of the European Commission.

REFERENCES

[1]. D. Ćirić et.al., Fusion Engineering and Design **86**, (2011) 509-512.
[2]. T. Kurki-Suonio et.al., Nuclear Fusion **49**, (2009) 095001.
[3]. J. Wesson, Nuclear Fusion **37**, (1997) pp. 577.
[4]. M. Romanelli, JET internal report JET-R(99)02.
[5]. P. Mantica et.al., this conference

Shot C	*Shot ILW*	*Type*
76899	*82794*	*hybrid high δ*
77154	*82722*	*hybrid low δ*
79441	*82806*	*baseline high δ*
77955	*83479*	*baseline low δ*

Table 1: List of discharges for NBI modelling

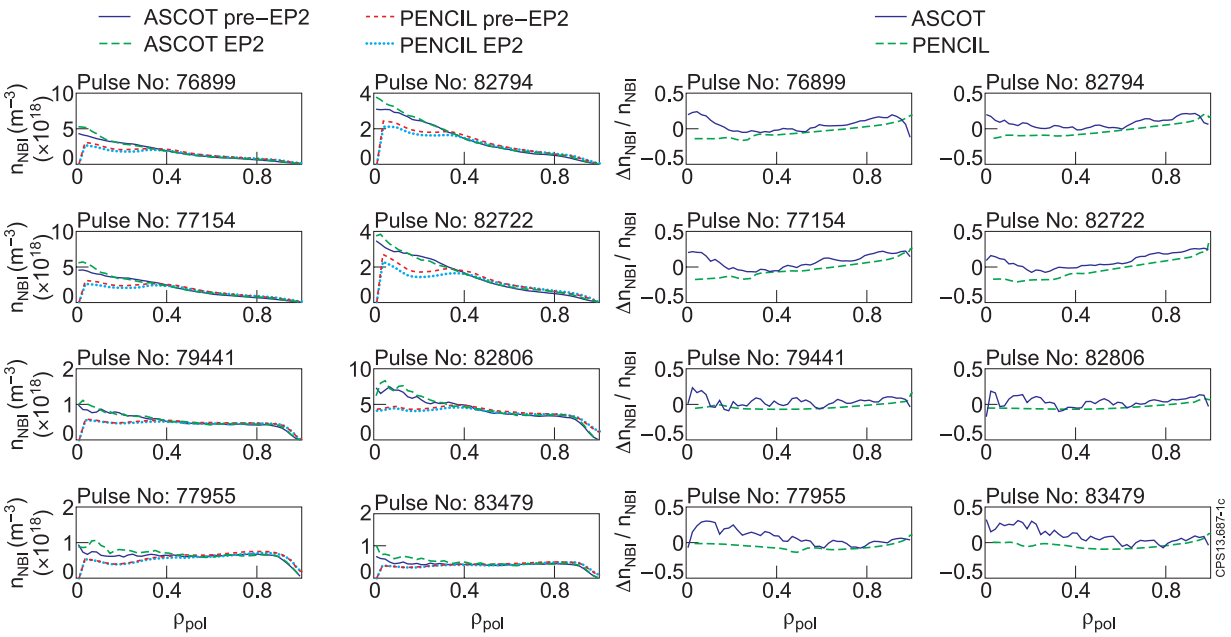

Figure 1: Comparison of beam ion deposition density, calculated by ASCOT and PENCIL for pre-EP2 and post-EP2 beams in C wall and ILW plasmas.

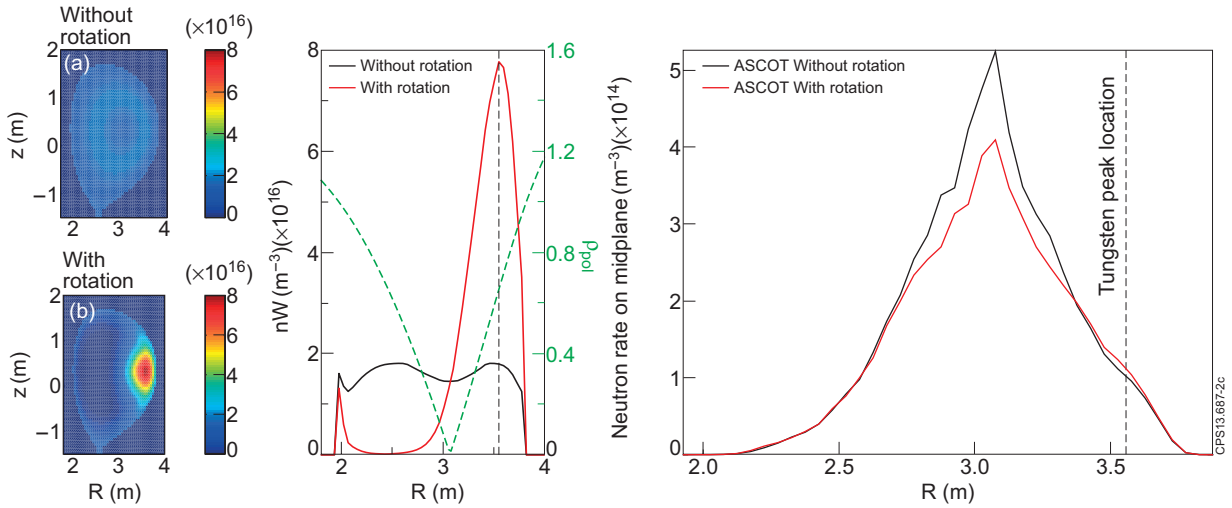

Figure 2: Simulation of tungsten asymmetry in a single time slice; (a) tungsten density without the effect of rotation (b) tungsten density with rotation (c) cross-section of tungsten density at midplane (d) simulated DD reaction rate at midplane.

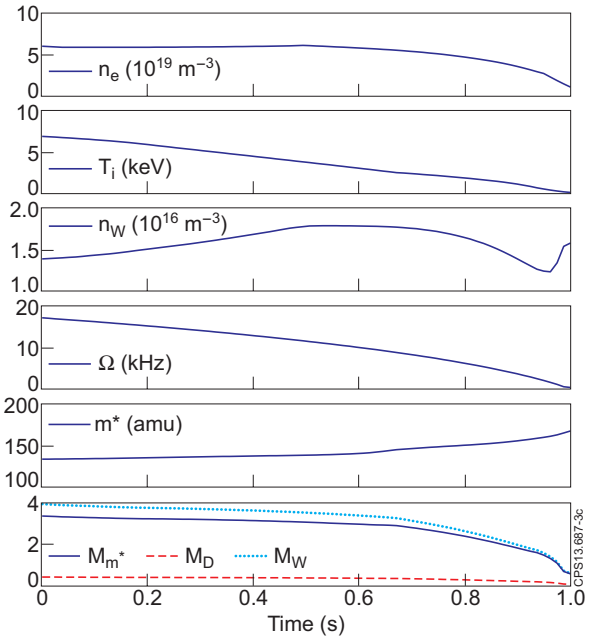

Figure 3: Flux-surface averaged profiles used in the calculation of the tungsten asymmetry in figure 2(b-c).

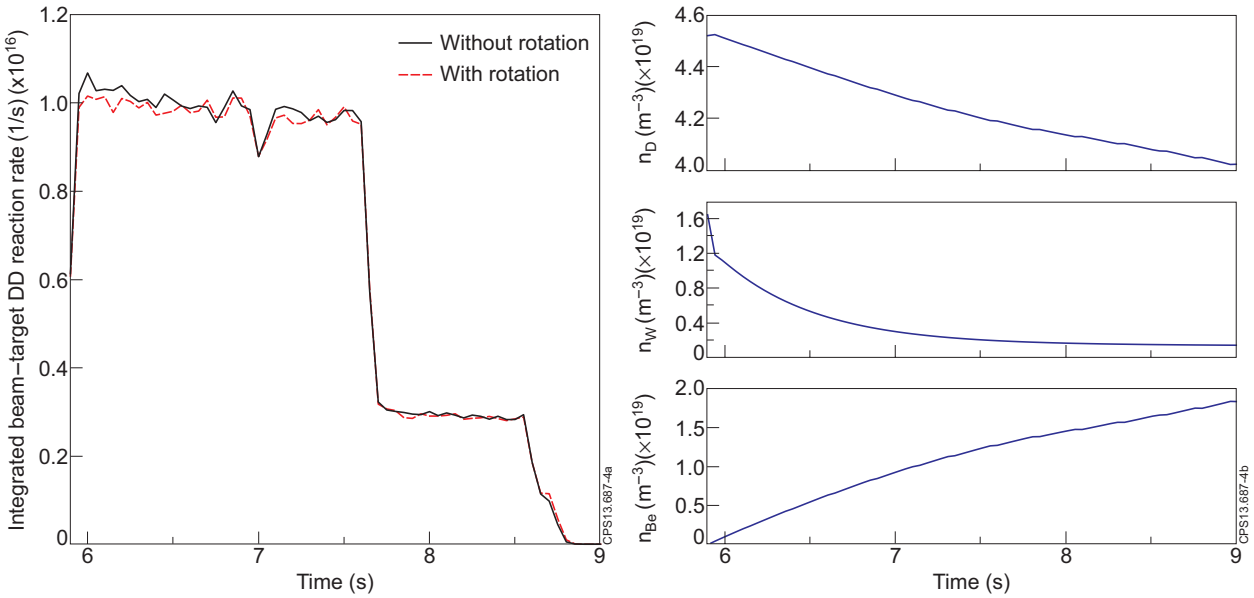

Figure 4: Time dependent simulation of tungsten asymmetry. On the left, the volume integrated DD reaction rate, with and without the effect of rotation on tungsten. On the right, the time evolution of the densities of D, W and Be.